

Anomalous elastic response of $\text{HoBa}_{2-x}\text{Ho}_x\text{Cu}_3\text{O}_{7-\delta}$ ceramic superconductors

A.K. Yahya^{a,*}, N.A. Hamid^b, R. Abd-Shukor^c, H. Imad^d

^a Faculty of Applied Sciences, Universiti Teknologi MARA, 40450 Shah Alam, Selangor, Malaysia

^b College of Engineering, Universiti Tenaga Nasional, 43009 Kajang, Selangor, Malaysia

^c School of Applied Physics, Universiti Kebangsaan Malaysia, 43600 Bangi, Selangor, Malaysia

^d Faculty of Science and Environmental Studies, Universiti Putra Malaysia, 43400 UPM Serdang, Selangor, Malaysia

Received 19 November 2003; received in revised form 11 December 2003; accepted 22 December 2003

Available online 10 May 2004

Abstract

Anomalous elastic response has been observed in superconducting $\text{HoBa}_{2-x}\text{Ho}_x\text{Cu}_3\text{O}_{7-\delta}$ ($x = 0$ and 0.15) from temperature dependent ultrasonic velocity measurements between 80 and 270 K. Longitudinal velocity of superconducting $\text{HoBa}_2\text{Cu}_3\text{O}_{7-\delta}$ ($T_{c\text{ zero}} \sim 89$ K) showed an anomaly around 230 K indicating a pronounced lattice stiffening. Superconducting $\text{HoBa}_{1.85}\text{Ho}_{0.15}\text{Cu}_3\text{O}_{7-\delta}$ ($T_{c\text{ zero}} \sim 70$ K) also showed a similar longitudinal velocity anomaly around the same temperature. No anomaly was observed for oxygen-reduced non-superconducting $\text{HoBa}_2\text{Cu}_3\text{O}_{7-\delta}$. Temperature dependent shear velocity profiles and absolute velocity measurements at 80 K are also reported and the influence of oxygen content on elastic properties is discussed.

© 2004 Elsevier Ltd and Techna Group S.r.l. All rights reserved.

Keywords: A. Powders: solid state reaction; B. Microstructure-final; D. Oxide superconductors; Elastic properties

1. Introduction

Ultrasonic investigation at low temperatures is useful in providing valuable information on various dynamic properties of materials. The ultrasonic method is sensitive to changes in elastic properties and can provide clues for better understanding of the phenomena of high-temperature superconductivity. Studies on $\text{REBa}_2\text{Cu}_3\text{O}_{7-\delta}$ (RE-rare earth) and other high-temperature superconductors showed several elastic anomalies near and above 200 K ([1,2] and references therein). The elastic anomalies above 200 K are observed to be related to the oxygen content and are interpreted to be caused by some form of oxygen ordering in the materials. The studies confirm the major role played by oxygen not only on superconductivity of high-temperature superconductors but also on its elastic properties. Nevertheless, the nature of the mechanisms which control the elastic anomalies remains an open question.

On the other hand, the effects of chemical substitutions on the physical and superconducting properties of $\text{REBa}_2\text{Cu}_3\text{O}_{7-\delta}$ have been extensively reported. Reasonable interest was focussed on occupancy of RE^{3+} at Ba-site of $\text{REBa}_2\text{Cu}_3\text{O}_{7-\delta}$ to investigate the importance of the atomic-site in the (1 2 3) structure [3–5]. However, the question still remains whether the magnetic RE^{3+} ions at the Ba-sites really have fatal effects on superconductivity. Although there are reports on the effect of chemical substitutions on absolute velocity values and temperature dependent velocity profiles of high-temperature superconductors the number is quite limited [6,7]. Thus, an ultrasonic study on $\text{RE}(\text{Ba}_{2-x}\text{RE}_x)\text{Cu}_3\text{O}_{7-\delta}$ would be of particular interest to provide further understanding on the importance and role played by the Ba-site.

This paper reports on the longitudinal ultrasonic wave velocity measurements in superconducting $\text{Ho}(\text{Ba}_{2-x}\text{Ho}_x)\text{Cu}_3\text{O}_{7-\delta}$ ($x = 0$ and 0.15) and non-superconducting $\text{HoBa}_2\text{Cu}_3\text{O}_{7-\delta}$ with the aim to investigating the effect of oxygen content and Ba-site substitution on the elastic properties of these materials. Results from electrical resistance (dc), powder X-ray diffraction (XRD) and microstructure

* Corresponding author. Tel.: +60-3-55444613; fax: +60-3-55444562.
E-mail address: ahmad191@salam.uitm.edu.my (A.K. Yahya).

investigations using scanning electron microscope (SEM) are also presented.

2. Experimental procedure

2.1. Samples preparation

The $\text{HoBa}_{2-x}\text{Ho}_x\text{Cu}_3\text{O}_{7-\delta}$ ($x = 0$ and 0.15) samples were prepared by mixing appropriate amounts of Ho_2O_3 , BaCO_3 and CuO powders with purity $\geq 99.99\%$. The materials were ground in a mortar then calcined in air at around 900°C for 48 h with several intermittent grindings and oven cooled. The powders were then pressed into pellets of 13 mm diameter and 2–3 mm thickness under a load of 8–9 tons. The pellets were sintered at the same temperature for 24 h and slow cooled to room temperature at 40°C/h . The oxygen-reduced non-superconducting sample was prepared by reheating the $\text{HoBa}_2\text{Cu}_3\text{O}_{7-\delta}$ sample at around 900°C for 30 min and quenching it immediately in liquid nitrogen.

2.2. Characterization

Electrical resistance (dc) measurements of the samples were carried out using the four-point-probe technique with silver paint contacts. The samples were also examined by X-ray powder diffraction with $\text{Cu K}\alpha$ radiation using Siemens D 5000 diffractometer. SEM micrographs were recorded using a JEOL model JSM 6400 scanning electron microscope.

The ultrasonic velocity was measured using a Matec 7700 system which utilizes the pulse-echo-overlap technique. The transducer was bonded on polished sample surface using Nonaq stopcock grease. Sound velocity was propagated along the direction of pressing using X-cut (longitudinal) or Y-cut (shear) transducer with a carrier frequency of 10 MHz. The velocity measurements were performed in an Oxford Instrument liquid nitrogen cryostat model DN 1711 and the temperature was changed at a rate of around 1 K/min during warming and cooling. No thermal expansion correction was made.

3. Results

3.1. Phase identification and electrical resistance measurements

Powder X-ray diffraction patterns (Fig. 1) showed all samples consist of essentially single phased (123) structure. Electrical resistance versus temperature measurements (Fig. 2) for $\text{HoBa}_2\text{Cu}_3\text{O}_{7-\delta}$ showed metallic normal state behavior with $T_{c\text{ zero}}$ of 89 K. $\text{HoBa}_{1.85}\text{Ho}_{0.15}\text{Cu}_3\text{O}_{7-\delta}$ exhibited less metallic normal state behavior with T_c of 70 K. Room temperature resistivity for $\text{HoBa}_{1.85}\text{Ho}_{0.15}\text{Cu}_3\text{O}_{7-\delta}$

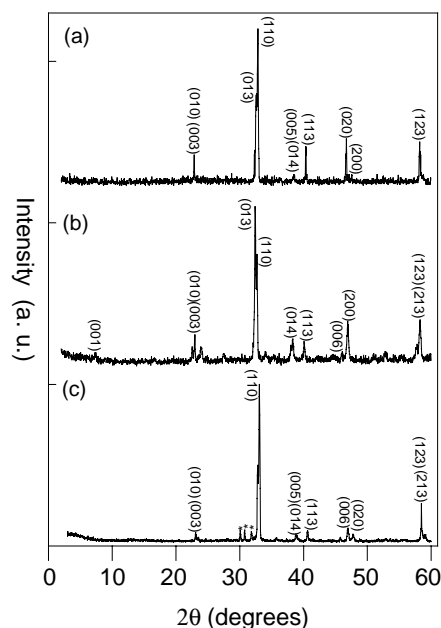


Fig. 1. X-ray powder diffractograms of (a) superconducting $\text{HoBa}_2\text{Cu}_3\text{O}_{7-\delta}$, (b) non-superconducting $\text{HoBa}_2\text{Cu}_3\text{O}_{7-\delta}$, and (c) $\text{HoBa}_{1.85}\text{Ho}_{0.15}\text{Cu}_3\text{O}_{7-\delta}$. Impurity peaks are indicated by asterisk (*).

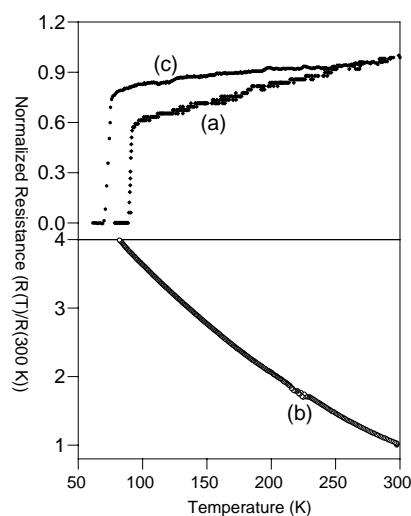


Fig. 2. Normalized resistance vs. temperature curve of (a) superconducting $\text{HoBa}_2\text{Cu}_3\text{O}_{7-\delta}$, (b) non-superconducting $\text{HoBa}_2\text{Cu}_3\text{O}_{7-\delta}$, and (c) $\text{HoBa}_{1.85}\text{Ho}_{0.15}\text{Cu}_3\text{O}_{7-\delta}$ samples.

shows a 80-fold increase compared to $\text{HoBa}_2\text{Cu}_3\text{O}_{7-\delta}$. Quenched $\text{HoBa}_2\text{Cu}_3\text{O}_{7-\delta}$ is non-superconducting down to 30 K and it is not expected to superconduct because of high resistivity value at room temperature. Table 1 shows the $T_{c\text{ zero}}$, $T_{c\text{ onset}}$, resistivity at 300 K, density and lattice parameters of all samples.

3.2. Ultrasonic velocity measurements

The absolute values of longitudinal and shear velocities at 80 K are tabulated in Table 2. The polycrystalline ceram-

Table 1

Values of critical temperature ($T_{c\text{zero}}$), onset critical temperature ($T_{c\text{onset}}$), room temperature resistivity, density and lattice parameters of (a) superconducting $\text{HoBa}_2\text{Cu}_3\text{O}_{7-\delta}$, (b) non-superconducting $\text{HoBa}_2\text{Cu}_3\text{O}_{7-\delta}$, and (c) $\text{HoBa}_{1.85}\text{Ho}_{0.15}\text{Cu}_3\text{O}_{7-\delta}$

Sample	$T_{c\text{zero}}$ (K)	$T_{c\text{onset}}$ (K)	Resistivity ($\text{m}\Omega\text{cm}$)	Density (g/cm^3)	Lattice parameters		
					a (\AA)	b (\AA)	c (\AA)
(a) $\text{HoBa}_2\text{Cu}_3\text{O}_{7-\delta}$	89	93	0.8	5.6	3.83	3.88	11.68
(b) $\text{HoBa}_2\text{Cu}_3\text{O}_{7-\delta}$	—	—	2.9×10^4	5.4	3.87	3.87	11.82
(c) $\text{HoBa}_{1.85}\text{Ho}_{0.15}\text{Cu}_3\text{O}_{7-\delta}$	70	77	6.4×10	5.3	3.87	3.88	11.68

Table 2

Longitudinal velocity (v_l), shear velocity (v_s), longitudinal modulus (C_L), shear modulus (μ), bulk modulus (B), Young's modulus (Y) and Debye temperature (θ_D) measured at 80 K of (a) superconducting $\text{HoBa}_2\text{Cu}_3\text{O}_{7-\delta}$, (b) non-superconducting $\text{HoBa}_2\text{Cu}_3\text{O}_{7-\delta}$, and (c) $\text{HoBa}_{1.85}\text{Ho}_{0.15}\text{Cu}_3\text{O}_{7-\delta}$

Sample	v_l (km/s)	v_s (km/s)	C_L (GPa)	μ (GPa)	B (GPa)	Y (GPa)	θ_D (K)
(a) $\text{HoBa}_2\text{Cu}_3\text{O}_{7-\delta}$	4.15	2.52	95.7	35.3	48.7	85.3	348
(b) $\text{HoBa}_2\text{Cu}_3\text{O}_{7-\delta}$	3.95	2.33	84.6	29.5	45.2	72.8	322
(c) $\text{HoBa}_{1.85}\text{Ho}_{0.15}\text{Cu}_3\text{O}_{7-\delta}$	4.55	2.49	109	32.8	65.8	84.4	347

ics can be treated as an isotropic material having two independent elastic stiffness moduli C_L ($= \rho v_l^2$) and μ ($= \rho v_s^2$), where C_L is the longitudinal modulus, μ is the shear modulus, ρ is the mass density, v_l is the longitudinal velocity and v_s is the shear velocity. The related elastic stiffness moduli, bulk modulus (B) and Young's modulus (Y) were determined using the measured ultrasonic wave velocity values. The acoustic Debye temperature (θ_D) was calculated using the standard formula:

$$\theta_D = \left(\frac{h}{k} \right) \left(\frac{3N}{4\pi V} \right)^{1/3} v_m$$

where h is the Planck constant, k is the Boltzmann constant, N is the number of mass point, V is the atomic volume and v_m is the mean velocity. The mean velocity is given by

$$\frac{3}{v_m^3} = \frac{1}{v_l^3} + \frac{2}{v_s^3}$$

The Debye temperature (θ_D) of superconducting $\text{HoBa}_2\text{Cu}_3\text{O}_{7-\delta}$ evaluated at 80 K is 348 K and is comparable to $\text{REBa}_2\text{Cu}_3\text{O}_{7-\delta}$ ($\text{RE} = \text{Y, Gd}$) superconductors [8,9]. Substitution of Ho for Ba in $\text{HoBa}_{1.85}\text{Ho}_{0.15}\text{Cu}_3\text{O}_{7-\delta}$ suppressed $T_{c\text{zero}}$ by 19 K but did not cause a large change in θ_D .

The reduction of oxygen content of $\text{HoBa}_2\text{Cu}_3\text{O}_{7-\delta}$ by quenching caused a decrease in both the v_l , v_s , related elastic moduli and θ_D (Table 2). On the other hand, the Ba-site substitution in $\text{HoBa}_{1.85}\text{Ho}_{0.15}\text{Cu}_3\text{O}_{7-\delta}$ caused an increase in v_l , C_L and B (Table 2) accompanied by a decrease in v_s , μ and Y .

Superconducting $\text{HoBa}_2\text{Cu}_3\text{O}_{7-\delta}$ showed a change in longitudinal velocity of 2.3% (Fig. 3a) between 80 and 270 K and a change in shear velocity of around 1.5% (Fig. 4a) between 80 and 205 K. Longitudinal velocity showed a change in slope around 230 K, below which, the velocity showed a large increase indicating pronounced lattice stiffening ten-

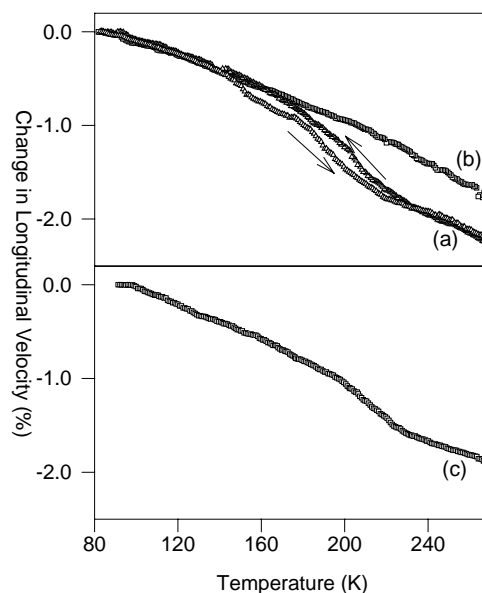


Fig. 3. Temperature dependence of longitudinal velocity for (a) superconducting $\text{HoBa}_2\text{Cu}_3\text{O}_{7-\delta}$, (b) non-superconducting $\text{HoBa}_2\text{Cu}_3\text{O}_{7-\delta}$, and (c) $\text{HoBa}_{1.85}\text{Ho}_{0.15}\text{Cu}_3\text{O}_{7-\delta}$.

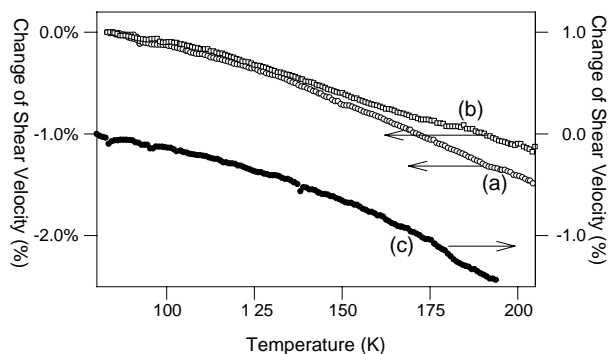


Fig. 4. Temperature dependence of shear velocity for (a) superconducting $\text{HoBa}_2\text{Cu}_3\text{O}_{7-\delta}$, (b) non-superconducting $\text{HoBa}_2\text{Cu}_3\text{O}_{7-\delta}$, and (c) $\text{HoBa}_{1.85}\text{Ho}_{0.15}\text{Cu}_3\text{O}_{7-\delta}$.

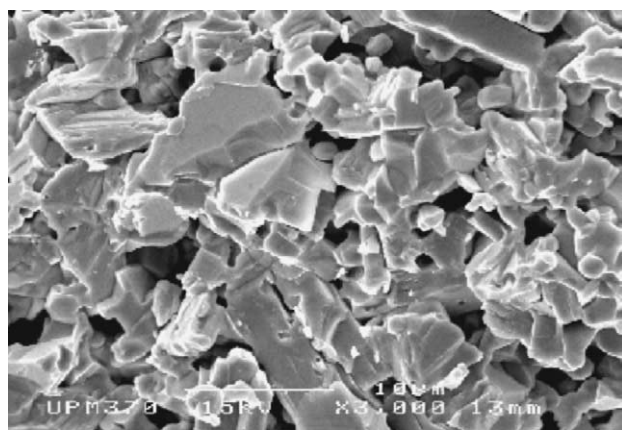
density. A longitudinal velocity hysteresis was observed between 140 and 230 K.

After quenching to reduce the oxygen content, non-superconducting $\text{HoBa}_2\text{Cu}_3\text{O}_{7-\delta}$ showed a change in longitudinal velocity of 1.8% (Fig. 3b) between 80 and 270 K and a change in shear velocity of around 1.2% (Fig. 4b) between 80 and 205 K. No velocity anomaly was observed for both modes. The longitudinal velocity hysteresis observed for superconducting $\text{HoBa}_2\text{Cu}_3\text{O}_{7-\delta}$ was not observed when oxygen content was reduced.

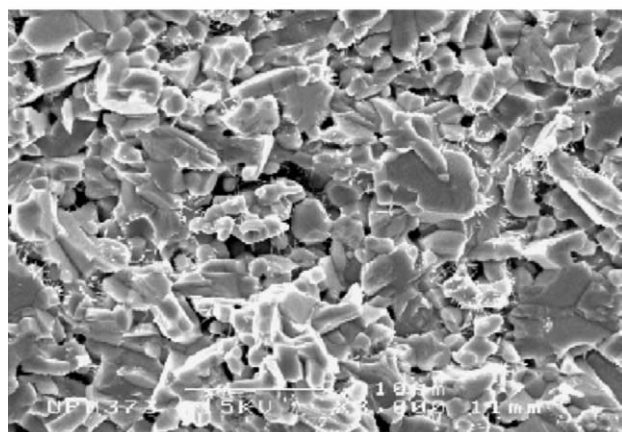
$\text{HoBa}_{1.85}\text{Ho}_{0.15}\text{Cu}_3\text{O}_{7-\delta}$ showed a change in longitudinal velocity of 2.0% between 80 and 270 K (Fig. 3c) and a change in shear velocity of around 1.5% between 80 and 195 K (Fig. 4c). Longitudinal velocity showed an anomalous change in slope around 230 K indicating pronounced lattice stiffening tendency. No longitudinal velocity hysteresis was observed.

3.3. Microstructure

SEM micrographs of the internal section of the samples showed irregular shaped grains accompanied by voids



(a)



(b)

Fig. 5. Scanning electron micrograph of (a) superconducting $\text{HoBa}_2\text{Cu}_3\text{O}_{7-\delta}$ and (b) $\text{HoBa}_{1.85}\text{Ho}_{0.15}\text{Cu}_3\text{O}_{7-\delta}$.

and pores. The estimated grain sizes for superconducting $\text{HoBa}_2\text{Cu}_3\text{O}_{7-\delta}$ and non-superconducting $\text{HoBa}_2\text{Cu}_3\text{O}_{7-\delta}$ were between 5 and 10 μm and no significant variation in microstructure is observed for the two samples. $\text{HoBa}_{1.85}\text{Ho}_{0.15}\text{Cu}_3\text{O}_{7-\delta}$ showed slightly smaller grains with an average grain size of about 4 μm . Fig. 5 shows the SEM micrographs of superconducting $\text{HoBa}_2\text{Cu}_3\text{O}_{7-\delta}$ and $\text{HoBa}_{1.85}\text{Ho}_{0.15}\text{Cu}_3\text{O}_{7-\delta}$.

4. Discussion

4.1. Absolute velocity at 80 K

The decrease in v_l and v_s (Table 2) upon quenching of $\text{HoBa}_2\text{Cu}_3\text{O}_{7-\delta}$ may not be due to major differences in porosity because the same pellet was used for preparation of the superconducting and non-superconducting samples. As such, the decrease in the longitudinal velocity observed for non-superconducting $\text{HoBa}_2\text{Cu}_3\text{O}_{7-\delta}$ may be caused by a volume dependent mechanism which involves reduction in the mean copper valence as a result of oxygen O(4) removal from the Cu–O chains during quenching. The reduction of average Cu valence caused an increase in ionic radius of Cu ions which acts to change some interatomic distances and bonding length. A reduction in the absolute values of ultrasonic velocities due to similar removal of oxygen have also been observed for $\text{REBa}_2\text{Cu}_3\text{O}_{7-\delta}$ (RE = Y, Gd) [9,10].

The increase in longitudinal velocity for $\text{HoBa}_{1.85}\text{Ho}_{0.15}\text{Cu}_3\text{O}_{7-\delta}$ (Table 2) may be due to cell volume change as a result of substitution of the smaller Ho^{3+} (ionic radius: 0.894 Å) for Ba^{2+} (ionic radius: 1.34 Å). The substitution may also have altered some interatomic distances and bonding lengths in $\text{HoBa}_2\text{Cu}_3\text{O}_{7-\delta}$ and this volume change was detected by the longitudinal phonons [11].

4.2. Effect of oxygen content and Ba-site substitution on 230 K elastic anomaly

A comparison of the temperature dependent velocity profiles between superconducting and non-superconducting $\text{HoBa}_2\text{Cu}_3\text{O}_{7-\delta}$ showed strong influence of oxygen content above 140 K for both modes. The 230 K longitudinal velocity anomaly in superconducting $\text{HoBa}_2\text{Cu}_3\text{O}_{7-\delta}$ could not be due to a structural transition since no structural anomaly is reported around 200 K. A possible explanation to the 230 K anomaly could be due to oxygen ordering in the sample. The temperature dependence of longitudinal velocity is dominated by vibrational anharmonicity at low temperatures but above 180 K, an oxygen-related mechanism dominates causing the 230 K anomaly. A similar velocity anomaly observed in $\text{YBa}_2\text{Cu}_3\text{O}_{7-\delta}$ around 200 K was suggested to be a first order phase transition involving oxygen ordering in the temperature range of 200–230 K [12]. Specific oxygen rearrangement patterns in Cu–O chains forming different orthorhombic superstructures have been suggested [12]. A

similar oxygen ordering mechanism may also cause the 230 K anomaly in $\text{HoBa}_2\text{Cu}_3\text{O}_{7-\delta}$ as orthorhombic superstructures have been observed in high-resolution electron microscopy studies of $\text{REBa}_2\text{Cu}_3\text{O}_7$ [13].

The absence of a similar velocity anomaly in non-superconducting $\text{HoBa}_2\text{Cu}_3\text{O}_{7-\delta}$ confirms its oxygen-related feature. It also shows a clear role of oxygen on the acoustic anomaly in agreement with previous reports for $\text{REBa}_2\text{Cu}_3\text{O}_{7-\delta}$ [7,14]. However, as previously suggested for Gd1113 [15], the absence of the anomaly in non-superconducting $\text{HoBa}_2\text{Cu}_3\text{O}_{7-\delta}$ may not simply be due to reduced oxygen content but the lack of oxygen ordering. A comparative study on oxygenated and partially oxygenated Y123 suggests that the anomaly is associated with long-range oxygen ordering in the Cu–O chains [16]. The disappearance of the longitudinal velocity hysteresis between 140 and 230 K upon oxygen reduction indicates the hysteresis may be associated with the twinned structure of the orthorhombic phase [17]. Microstructure of the samples is not likely to cause the hysteresis since SEM micrographs of superconducting $\text{HoBa}_2\text{Cu}_3\text{O}_{7-\delta}$ (Fig. 5a) and non-superconducting $\text{HoBa}_2\text{Cu}_3\text{O}_{7-\delta}$ (figure not shown) showed no significant variation in their microstructures.

Observation of a similar longitudinal velocity anomaly for $\text{HoBa}_{1.85}\text{Ho}_{0.15}\text{Cu}_3\text{O}_{7-\delta}$ suggests that Ba-site substitution does not affect oxygen ordering in CuO chains. The suppression of T_{c0} and the large increase in room-temperature resistivity due to Ho^{3+} substitution for Ba^{2+} indicate lowering of charge carrier concentration. However, our study shows that although Ho^{3+} substitutions at the Ba-sites have fatal effects on superconductivity, the acoustic anomaly is not affected by the lower charge carrier concentration. As such, there may be no direct relationship between the anomaly and charge carrier concentration. The absence of any velocity hysteresis for $\text{HoBa}_{1.85}\text{Ho}_{0.15}\text{Cu}_3\text{O}_{7-\delta}$ may be due to absence of twins as a result of the Ba-site substitution. However, it may also be due to smaller average grain size of the $\text{HoBa}_{1.85}\text{Ho}_{0.15}\text{Cu}_3\text{O}_{7-\delta}$ sample (Fig. 5b) compared to superconducting $\text{HoBa}_2\text{Cu}_3\text{O}_{7-\delta}$ (Fig. 5a).

5. Conclusions

We have performed ultrasonic longitudinal and shear velocity measurements in $\text{HoBa}_{2-x}\text{Ho}_x\text{Cu}_3\text{O}_{7-\delta}$ ($x = 0, 0.15$) ceramics. Oxygen-related elastic anomalies were observed around 230 K in superconducting $\text{HoBa}_2\text{Cu}_3\text{O}_{7-\delta}$ and $\text{HoBa}_{1.85}\text{Ho}_{0.15}\text{Cu}_3\text{O}_{7-\delta}$. In the absence of any reported structural changes in the vicinity, the anomalies are attributed to some form of oxygen ordering involving different orthorhombic superstructures. Observation of the 230 K anomaly in $\text{HoBa}_{1.85}\text{Ho}_{0.15}\text{Cu}_3\text{O}_{7-\delta}$ also suggests that Ba-site substitution by Ho^{3+} does not affect oxygen ordering in CuO chains.

Acknowledgements

The authors would like to thank Amri Faisal for some of the lab work. This research has been supported by Bureau of Research and Consultancy, Universiti Teknologi MARA. Project code: 10248.

References

- [1] S. Hoen, L.C. Bourne, M. Kim Choon, A. Zettl, Elastic response of polycrystalline and single-crystal $\text{YBa}_2\text{Cu}_3\text{O}_7$, *Phys. Rev. B* 38 (16) (1988) 11949–11951.
- [2] T.L. Laegreid, K. Fossheim, F. Vassendeu, Elastic and thermal behaviour of ceramic high- T_c superconductors studied by ultrasound, vibrating reed and specific heat measurements, *Physica C* 153–155 (1988) 1096–1099.
- [3] M.J. Kramer, S.I. Yoo, R.W. McCallium, Y.B. Yelon, H. Xie, P. Allenspach, Hole filling, charge transfer and superconductivity in $\text{Nd}_{1+x}\text{Ba}_{2-x}\text{Cu}_3\text{O}_{7+}$, *Physica C* 219 (1994) 145–155.
- [4] K.M. Pansuria, D.G. Kuberkar, R.G. Kulkarni, Influence of hole filling by La and hole doping by Ca on the superconductivity of $\text{ErBa}_2\text{Cu}_3\text{O}_{7-\delta}$, *Supercond. Sci. Technol.* 10 (1997) 831–835.
- [5] H.A. Blackstead, J.D. Dow, Role of Ba-site Pr in quenching superconductivity of $\text{Y}_{1-y}\text{Pr}_y\text{Ba}_2\text{Cu}_3\text{O}_x$ and related materials, *Phys. Rev. B* 51 (1995) 11830–11837.
- [6] R. Abd-Shukor, Ultrasonic shear velocity anomalies in bulk thallium-1212 high temperature superconductor, *Mod. Phys. Lett. B* 11 (1997) 359–365.
- [7] A.K. Yahya, R. Abd-Shukor, Ultrasonic velocity measurements on superconducting and non-superconducting $\text{TiSr}_2\text{Ca}_{1-x}\text{Pr}_x\text{Cu}_2\text{O}_{7-\delta}$, *Physica C* 314 (1999) 117–124.
- [8] J. Dominec, Ultrasonic and related experiments in high T_c -superconductors, *Supercond. Sci. Technol.* 6 (1993) 153–172.
- [9] Q. Wang, G.A. Saunders, D.P. Almond, M. Cankurtaran, K.C. Goretti, Elastic and nonlinear acoustic properties of $\text{YBa}_2\text{Cu}_3\text{O}_{7-\delta}$ ceramics with different oxygen contents, *Phys. Rev. B* 52 (5) (1995) 3711–3725.
- [10] D.P. Almond, Q. Wang, J. Freestone, E.F. Lambson, B. Chapman, G.A. Saunders, An ultrasonic study of superconducting and non-superconducting $\text{GdBa}_2\text{Cu}_3\text{O}_{7-\delta}$, *J. Phys.: Condens. Matter* 1 (1989) 6853–6864.
- [11] C. Fanggao, M. Cankurtaran, G.A. Saunders, D.P. Almond, P.J. Ford, A. Al-Kheffaji, The effects of quenching and lead substitution on the ultrasonic wave velocity and attenuation in bismuth cuprate high T_c superconductors, *Supercond. Sci. Technol.* 3 (1990) 546–555.
- [12] G. Ceder, M. Asta, D. de Fontaine, Computation of the OI–OII–OIII phase diagram and local oxygen configurations for $\text{YBa}_2\text{Cu}_3\text{O}_z$ with z between 6.5 and 7, *Physica C* 177 (1991) 106–114.
- [13] T. Kerkels, H. Zou, G. Van. Tendeloo, D. Wagener, M. Buchgeister, S.M. Hosseini, P. Herzog, Ortho II structure in $\text{ABa}_2\text{Cu}_3\text{O}_{7-\delta}$ compounds ($A = \text{Er}, \text{Nd}, \text{Pr}, \text{Sm}, \text{Yb}$), *Physica C* 196 (1992) 363–368.
- [14] M. Cankurtaran, G.A. Saunders, Q. Wang, H. Celik, Anharmonic contribution to the temperature dependence of the ultrasonic wave velocity in sintered $\text{YBa}_2\text{Cu}_3\text{O}_{7-x}$ ceramics with different oxygen contents, *Supercond. Sci. Technol.* 8 (1995) 811–815.
- [15] A.K. Yahya, A.K. Koh, R. Abd-Shukor, Comparative study of ultrasonic velocity in differently annealed and quenched $\text{GdBaSrCu}_3\text{O}_{7-\delta}$ superconductors, *Phys. Lett. A* 259 (3/4) (1999) 295–301.
- [16] A.R. Anderson, M. Murakami, K. Russell, G.J. Nagashima, Evidence of structural change in TSMG Y123 at 225 K, *Physica C* 306 (1998) 15–20.
- [17] D.P. Almond, G.A. Saunders, E.F. Lambson, Ultrasonic evidence indicating $\text{YBa}_2\text{Cu}_3\text{O}_{7-x}$ to be a pseudoplastic material, *Supercond. Sci. Technol.* 1 (1988) 163–166.